# Macromolecular Stereochemistry: Helical Sense Preference in Optically Active Polyisocyanates. Amplification of a Conformational Equilibrium Deuterium Isotope Effect

**Shneior Lifson,*,† Christopher Andreola,‡ Norman C. Peterson,‡ and Mark M. Green*,‡,§**

*Contribution from the Department of Chemical Physics, Weizmann Institute of Science, Rehovol 76100, Israel, and Department of Chemistry and Polymer Research Institute, Polytechnic University, 333 Jay Street, Brooklyn, New York 11201.* *Received February 2, 1989*

**Abstract:** The qualitative model of a chirally perturbed polyisocyanate chain, with long helical sequences separated by helical sense reversals, has been interpreted quantitatively by statistical thermodynamics. The change of the specific optical rotation with temperature depends on the following: The energy of a helix sense reversal, $E_r$; the energy difference per monomer unit between the opposing helical senses, $2E_h$; the degree of polymerization, $N$. Three cases of dynamic equilibrium are considered: (1) Equilibrium between purely right-handed (P) and purely left-handed (M) short polymers; (2) equilibrium between many long alternating P and M helical sequences, separated by helix reversal states, in a very long polymer chain; (3) the general case of polymers of any length, including (1) and (2) as special cases. Calculations of the relationship between optical activity $[\alpha]_D$ and temperature prove that both cases 2 and 3 make an excellent fit to the corresponding measurements on poly-((*R*)-1-deuterio-*n*-hexyl isocyanate) of $M_W$ 870 000, in dilute chloroform and hexane solutions. In this fit of the experimental data to the theory, cases 2 and 3 differ somewhat, yielding values of $2E_h$ and $E_r$ near to 1 and 4000 cal/mol. The results confirm a cooperative model proposed to account for the unusual sensitivity of this polymer to asymmetric deuterium substitution and yield the energy bias of the isotope effect, which would otherwise be extremely difficult to measure. The calculated average lengths of helical sequences, evaluated from $E_r$, are too large to attribute the long-known flexibility of high molecular weight poly(*n*-alkyl isocyanates) to kinks at the reversals between otherwise stiff helical segments. Consequently the present results support strongly, though indirectly, the model of smooth bending with the global dimensions of these polymers dominated by local segmental motion.

In general, in the dissolved or molten state, a variety of local conformations are accessible to synthetic polymers, leading to their well-known random-coil global properties[1,2] which distinguish these polymers from those of biological interest where only a few allowed conformations are the rule.[3] Among the relatively few synthetic polymers that are conformationally restricted on a local level, polyisocyanates, first created by Du Pont chemists almost 30 years ago,[4] form a still rarer subset maintaining a stable extended helix in dilute solution.

The polyisocyanates, especially with *n*-alkyl pendant groups, have been the subject of a large literature concerned with their structure.[5] In contrast to random-coil polymers, the previous work[5] shows poly(*n*-alkyl isocyanates) to exhibit an approximately linear relationship between molecular weight and radius of gyration or dipole moment, a relationship that gradually decays toward the random-coil properties at high molecular weight. This is characteristic of wormlike chains[5,6] and leads to the inevitable question of what is the structural source of the accumulated flexibility.[6] Different points of view have assigned the flexibility either to smooth bending of the stiff helix, arising from local segmental motion, or to changes in chain direction associated with helix reversals.[7-10] These conformational questions,[7-10] which we are able to answer in the work described below, relate also to the liquid crystal forming characteristics of poly(*n*-alkyl isocyanates).[11]

In contrast to polypeptides, which also form extended helical conformations in solution,[3] polyisocyanates lack chirality in the monomeric precursors. This stereochemical distinction causes the polyisocyanates to adopt left- (M) and right-handed (P) helical conformations with equal probability. Goodman and Chen[12] first took the opportunity offered by the pendant group in allowing incorporation of stereogenicity. They synthesized polyisocyanates from two optically active monomers and found exceptionally high optical activities, associated with the recurring amide group chromophore, centered in the ultraviolet region. This observation very reasonably implied that the left- and right-handed helices, now cast into diasteromeric states, were no long equally populated.[13,14]

A particularly interesting member of the family of polyisocyanates synthesized from chiral monomers is poly((*R*)-1-deuterio-*n*-hexyl isocyanate) **1**.[15] Although the chiral perturbation

† Weizmann Institute of Science.
‡ Polytechnic University.
§ Address requests for reprints to this author.

(1) Flory, P. J. *Principles of Polymer Chemistry*; Cornell Unversity Press: Ithaca, NY, 1953; Chapter X, pp 399ff.
(2) Bailey, R. T.; North, A. M.; Pethrick, R. A. *Molecular Motion in High Polymers*; Clarendon Press: Oxford, England, 1981; Chapters 1, 4. Bovey, F. A. *Chain Structure and Conformation of Macromolecules*; Academic Press: NY, 1982; Chapter 7, pp 185ff.
(3) Cantor, C. R.; Schimmel, P. R. *Biophysical Chemistry, Part 1, The Conformation of Biological Macromolecules*; W. H. Freeman & Co.: San Francisco, CA, 1980.
(4) Shashoua, V. E.; Sweeney, W.; Tietz, R. F. *J. Am. Chem. Soc.* **1960**, *82*, 866.
(5) A critical review is: Bur, A.; Fetters, L. J. *Chem. Rev.* **1976**, *76*, 727. See also: Berger, M. N.; Tidswell, B. M. *J. Polym. Sci., Polym. Symp.* **1973**, *No. 42*, 1063.
(6) Recent papers with references to the large prior literature are: Itou, T.; Chikiri, H.; Teramoto, A.; Aharoni, S. M. *Polym. J.* **1988**, *20*, 143. Kuwata, M.; Murakami, H.; Norisuye, T.; Fujita, H. *Macromolecules* **1984**, *17*, 2731.
(7) Bur, A. J.; Roberts, D. E. *J. Chem. Phys.* **1969**, *51*, 406.
(8) Tonelli, A. E. *Macromolecules* **1974**, *7*, 628.
(9) Cook, R. *Macromolecules* **1987**, *20*, 1961.
(10) Mansfield, M. L. *Macromolecules* **1986**, *19*, 854.
(11) Leading references may be found in: Itou, T.; Teramoto, A. *Macromolecules* **1988**, *21*, 2225. Bianchi, E.; Ciferri, A.; Conio, G.; Krigbaum, W. R. *Polymer* **1987**, *28*, 813. Aharoni, S. H. In *Interrelations Between Processing Structure and Properties of Polymeric Materials, Materials Science Monograph*; Leferis, J. C., Theorcaris, P. S., Eds.; 1984; Vol. 21, pp 343ff.
(12) Goodman, M.; Chen, S. *Macromolecules* **1970**, *3*, 398; *Ibid.* **1971**, *4*, 625.
(13) Green, M. M.; Gross, R. A.; Cook, R.; Schilling, F. C. *Macromolecules* **1987**, *20*, 2636.
(14) Green, M. M.; Gross, R. A.; Crosby, C. C., III; Schilling, F. C. *Macromolecules* **1987**, *20*, 992.
(15) Green, M. M.; Andreola, C.; Muñoz, B.; Reidy, M. P.; Zero, K. *J. Am. Chem. Soc.* **1988**, *110*, 4063. For a related finding see: Green, M. M.; Reidy, M. P.; Johnson, R. D.; Darling, G.; O'Leary, D. J.; Willson, G. *J. Am. Chem. Soc.* **1989**, *111*, 6452.

0002-7863/89/1511-8850$01.50/0 

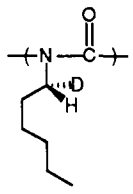

1

favoring one helical sense in **1** is driven only by the difference between hydrogen and deuterium, the strong temperature-dependent optical activity and circular dichroism suggest a large preference for one of the helical senses.[15] The fact that a very small energy difference per deuterium between diastereomers produces a significant helical excess was attributed to a cooperative effect, with the energy difference per monomer unit suggested to be multiplied by the large number of monomer units between helix reversals.[15] The polymer, according to this idea, would serve as an amplifier of the monomeric unit isotope effect. It was apparent that a quantitative analysis of these phenomena should yield important information to both test this idea and reveal details associated with the polymer conformation. This stimulated the present theoretical and experimental work.

Based on the conformational picture of polyisocyanates drawn above,[5,6] the behavior of these polymers is determined by three parameters. One is the energy of a helical sense reversal, $E_r$, relative to the helical state, the latter being the lowest energy state of a polyisocyanate chain. Reversals occur by thermal agitation, and the chain's stiffness is evidence that reversals are rare, i.e., that the energy of reversal is large.

The second parameter characterizes polyisocyanates with a preference for one helical sense. This is the energy difference, $\Delta E_h$, between the right-handed and left-handed conformations of each monomer unit. Since in the case of **1** this depends only on an isotopic distinction, it is necessarily small. Thus, the dynamic equilibrium of the poly((*R*)-1-deuterio-*n*-hexyl isocyanate) is determined by the interplay of a large energy of helical sense reversal and a small difference per monomer unit between the helical senses.

The third parameter is the molecular weight or degree of polymerization, $N$. Its role in understanding the conformational properties of polyisocyanates is exceptional because of the stiffness of the chain and the rarity of helix reversals. A chain is "short" if it contains no helix reversals. A long chain contains numerous, though long, alternating helical sequences. The intermediate case of polymers whose length is commensurable with the average dynamic length of the helical sequences is of particular interest. It may exhibit optical and dynamic properties that are different from those of the two extremes. It requires a general theory that contains the short and long polymers as special cases and determines their ranges of validity.

In the theoretical section we treat the short, long, and intermediate cases in that order. The section on comparison of experiment and theory discusses polyisocyanate **1** of weight average degree of polymerization $N$ equal to 6800 dissolved in chloroform and in hexane. Its optical rotation increases ~3-fold over the temperature range from +60 to −20 °C. Fitting the theoretical parameters by least squares shows an excellent match for the cases of long and intermediate chains. The value of $\Delta E_h$, in the range of 1 cal/mol, is too tiny to be interpreted by any current theoretical methods. The value of $E_r$, of the order of 4000 cal/mol, implies very long helical sequences. If these sequences were absolutely stiff, the observed dimensional and dipole moment properties of long polyisocyanates could not be explained. Therefore our results favor the model of smooth bending, a model in which conformational properties are dominated by local segmental motions.[9,10]

A further comment is warranted on polyisocyanates in relation to the extensively studied polypeptides, which also form extended helical conformations, particularly in nonpolar solvents. While the polyisocyanate residue is highly rigid, the amino acid residue is highly flexible. While the helices of polyisocyanates are intrinsically stable, and are nucleated by helix reversal, the helices of polypeptides are stabilized cooperatively by intramolecular hydrogen bonds. Notwithstanding these differences, both classes of polymers exhibit helical structures that are maintained by dynamic equilibrium between microscopic states and are therefore subject to similar statistical thermodynamic analysis.

**Statistical Mechanical Theory of Helical Polyisocyanates.** Let us first consider briefly polymers constructed from achiral monomers, whose P (right-handed) and M (left-handed) helices are equally probable, and the macroscopic system is racemic. In short polymers, there is an equal number of purely P and purely M chains. In long polymers the P and M sequences are separated by helix reversal conformations that terminate one helical sequence and initiate the next helical sequence of opposite sense. We shall attribute such reversals to a single monomer unit for the sake of simplicity in the absence of contrary evidence. In any event, whether the reversal conformation is focused on a single monomer unit or on two to three consecutive ones makes no difference to the analysis.

The average length of a helical sequence, $\bar{l}$, is given by the relative abundance of helical and reversal monomer units

$$\bar{l} = n_h/n_r \tag{1}$$

and is determined by the energy, $E_r$, of the reversal conformation relative to the helical conformation (the latter being chosen as the reference of energy zero). By Boltzmann distribution, through eq 1,

$$\bar{l} = \exp(E_r/RT) \tag{2}$$

where $RT$ is the thermal energy. Note that $\bar{l}$ is very sensitive to $E_r$. For example, at room temperature $RT$ = 0.6 kcal/mol), $E_r$ = 3 kcal/mol yields $\bar{l} \sim 150$, while $E_r$ = 5 kcal/mol yields $\bar{l} \sim$ 4160.

Consider next polyisocyanate polymers prepared from chiral nonracemic monomer units with side-chain stereocenters. In general, each stereocenter may interact with its neighbors, with the backbone of the chain, or both, such that the energy of interaction is different for P (right-handed) and M (left-handed) helical conformations. Taking the average of such interactions as the reference value of energy, and assuming the M conformation as more stable, the molar interaction energies of the M and P monomers may be denoted by $-E_h$, and $+E_h$, respectively, and the difference between them, $\Delta E_h$, is then $2E_h$. Even an extremely small value of $E_h$ may cause an uneven distribution of M and P helical states, since the distribution would be determined by the energy difference per sequence rather than per monomer.[15] The laws of distribution are, however, very different for short and long polymers, as we shall see below.

The uneven distribution of P and M helical states in the polyisocyanates is the source of the contribution of the backbone of the polymer to its optical rotation. In the following we derive the optical rotation, $[\alpha]$, as a function of the temperature, $T$, and the degree of polymerization, $N$. The energy difference between P and M helical states, $\delta E_h$, and the energy of reversal, $E_r$, may then be obtained by comparison of theory and experiment.

The statistical thermodynamic theory presented here is derived by the "sequence generating functions" method of evaluating the observable properties of polymers in general.[16] The method is adapted to our present subject with the particular purpose of interpreting the optical rotation of poly((*R*)-1-deuterio-*n*-hexyl isocyanate) **1**, whose optical rotation is assumed to be solely due to helical excess. However, the theory is valid for other similar polymers.

The basic concepts of the theory are the statistical weights of the different states that each monomer can acquite. Each monomer unit is assumed to exist in either one of three microscopic states: M helix, P helix, and reversal from one helical sense to the other (the states of reversal from P to M and vice versa are obviously the same). These states are assigned statistical weights $u_M$, $u_P$, and $v$, respectively, which represent their relative probabilities of occurrence according to the Boltzmann distribution law:

(16) Lifson, S. *J. Chem. Phys.* **1964**, *40*, 3705.

$$u_M = \exp(+E_h/RT) \qquad u_P = \exp(-E_h/RT)$$
$$v = \exp(-E_r/RT) \tag{3}$$

assuming that the energies $-E_h$ and $+E_h$ are attributed to M and P helices, respectively.

Once the weights $u_M$, $u_P$, and $v$ are defined, the statistical weight of any microscopic state of a polymer chain of length $N$ is obtainable, to a very good approximation, as a product of these weights. The sum of the statistical weights of the whole chain over all its microscopic states is the partition function $Z_N$. Any observable average property of the polymer chain is obtained from $Z_N$ by standard methods of statistical thermodynamics.

The average numbers of monomer units of opposite helicity, $n_M$ and $n_P$, respectively, and of reversal monomers, $n_V$ are

$$n_M = \partial \ln Z_N/\partial \ln u_M \qquad n_P = \partial \ln Z_N/\partial \ln u_P$$
$$n_V = \partial \ln Z_N/\partial \ln v \tag{4}$$

Since each helical sequence is initiated by a single reversal monomer, the average length $l_M$ of an M sequence is the number of M monomer units, $n_M$, divided by the number of M-helical sequences, $n_v/2$, and similarly for $l_P$. Consequently, the helical lengths and their ratio $r$ are obtain from $Z_N$ by

$$l_M = 2(u_M\partial Z_N/\partial u_M)/(v\partial Z_N/\partial v)$$
$$l_P = 2(u_P\partial Z_N/\partial u_P)/(v\partial Z_N/\partial v) \tag{5}$$
$$r = (u_M\partial Z_N/\partial u_M)/(u_P\partial Z_N/\partial u_P)$$

The specific optical rotation $[\alpha]$ is proportional to the relative excess of monomers of one helical sense over the other. It is obtained from $n_M$ and $n_P$ by

$$[\alpha] = [\alpha]_m\frac{n_M - n_P}{n_M + n_P} = [\alpha]_m\frac{r-1}{r+1} = [\alpha]_M\frac{u_M\partial Z_N/\partial u_M - u_P\partial Z_N/\partial u_P}{u_M\partial Z_N/\partial u_M + u_P\partial Z_N/\partial u_P} \tag{6}$$

where $[\alpha]_m$ is the specific optical rotation in the limit $n_{P\to 0}$.

There are several methods to derive $Z_N$. The derivation of $Z_N$ by the sequence generating functions method[16,17] is presented in the Appendix.

We shall present the statistical thermodynamic theory of optical rotation of polyisocyanates on three levels. First, we shall discuss the case of small $N$ and big $E_r$, where the calculated average length of a helical sequence, $\bar{l}$, given by eq 2, is longer than $N$. In this case, each polymer molecule is either purely M helical or purely P helical; $[\alpha]$ depends on $E_h$ and $N$, but is independent of $E_r$.

Second, we shall discuss the other extreme case, that of very long polymers, where $N \gg \bar{l}$. In this case, $[\alpha]$ depends on $E_h$ and $E_r$, but is independent of $N$.

Finally, we shall discuss the general case, where $[\alpha]$ is a function of $E_h$ and of both $N$ and $E_r$. This case covers the whole range of values of $N$ and $E_r$ and yields the first and second cases as limiting cases.

**Case 1: Short Polymers.** This case is simple and straightforward and does not require the elaborate statistical theory of polymer chains. It is considered here for two reasons. First, it is the best tool for the analysis of data within its range of validity. Second, the relation between the cases is of intrinsic theoretical interest.

Let $n_M$ and $n_P$ be the numbers (or molar concentrations) of purely M and of purely P helical polymers, respectively. The ratio, $r = n_M/n_P$ is given by the Boltzmann distribution

$$r = \exp(\pm 2E_hN/RT) \tag{7}$$

where + or − depends on whether the M or the P state is the one of lower energy.

(17) Schellman, J. A. In *Molecular Structure and Dynamics, Lectures on Biological and Chemical Physics*; Balaban, M., Ed.; Balaban International Services: Philadelphia, Jerusalem, 1980.

The specific optical rotation of the solution is determined by the relative abundance of helical states of one kind over the other, namely

$$[\alpha] = [\alpha]_m\frac{n_M - n_P}{n_M + n_P} = [\alpha]_m\frac{r-1}{r+1} = [\alpha]_m\frac{1 - \exp(-2E_hN/RT)}{1 + \exp(-2E_hN/RT)} \tag{8}$$

Equation 8 can also be presented as

$$\ln\frac{[\alpha]_m + [\alpha]}{[\alpha]_m - [\alpha]} = \ln r = 2E_hN/RT \tag{9}$$

The range of validity of eq 9 can be conveniently tested by experiment since it predicts $\ln r([\alpha])$ to be proportional to both $N$ and $1/T$.

**Case 2: Long Polymers.** In the limit of very long polymers the partition function is given (see Appendix, eq A14–A16) by

$$Z_N = x_1^N \qquad x_1 = \tfrac{1}{2}(u_M + u_P) + w$$
$$w = (\delta u^2 + v^2)^{1/2} \qquad \delta u = (u_M - u_P)/2 \tag{10}$$

Any observable property that is derivable from $Z_N$ can be derived in this case from $x_1$, which represents the partition function per monomer unit. In particular, the quantities $n_M$, $n_P$, $l_M$, $l_P$, $r$, and $[\alpha]$ are obtained from the partial derivatives of $x_1$:

$$\partial x_1/\partial u_M = \tfrac{1}{2} + \delta u/2w \qquad \partial x_1/\partial u_P = \tfrac{1}{2} - \delta u/2w$$
$$\partial x_1/\partial v = v/w \tag{11}$$

Let us examine the quantities in eq 10 and 11. If the energies of M and P helical monomers are very small, which is certainly the case in poly((*R*)-1-deuterio-*n*-alkyl isocyanate), then

$$\delta u \approx E_h/RT \ll 1 \qquad u_M \sim u_P \sim 1 \tag{12}$$

and since $v$ is also assumed to be very small, so is $w$. By its definition $w$ resembles the length of a vector with $\delta u$ and $v$ components. The balance between $v$ and $\delta u$ varies with temperature since $\delta u$ is proportional to $1/RT$ while $v$ varies exponentially with $1/RT$.

The average lengths $l_M$ and $l_P$ are obtained from eq 5 by use of eq 11 and 12:

$$l_M = u_M(w + \delta u)/v^2 \approx (w + \delta u)/v^2$$
$$l_P = u_P(w - \delta u)/v^2 \approx (w - \delta u)/v^2 \tag{13}$$

The ratio between the number of M and P residues, namely, their relative distribution, equals the ratio $l_M/l_P$ and is given by

$$r = (w + \delta u)/(w - \delta u) \tag{14}$$

This relative distribution is substantially different from that in case 1, given by eq 7.

The geometric and arithmetic means of the helical lengths are obtained from eq 13.

$$\bar{l} = (l_Ml_P)^{1/2} = 1/v \qquad \langle l\rangle = (l_M + l_P)/2 = w/v^2 \tag{15}$$

Note that $\bar{l}$ is independent of $\delta u$, namely, of any diastereomeric energy difference between P and M helical sequences.

In view of eq 15 and 12, the ratio $\delta u/v$ can be interpreted as half the energy difference (in $RT$ units) between M and P helical sequences of the same (geometric mean) length

$$\delta u/v = \bar{l}\delta u = \bar{l}E_h/RT = \bar{l}\Delta E_h/2RT \tag{16}$$

The specific optical rotation, $[\alpha]$, is obtained from eq 5, 6, and 13.

$$[\alpha] = [\alpha]_m\frac{(w + \delta u) - (w - \delta u)}{(w + \delta u) + (w - \delta u)} = [\alpha]_m\delta u/w \tag{17}$$

Equation 17 is transformed, by dividing both its numerator and denominator by $v$ and using eq 10, to a function of the single parameter $\bar{l}\delta u$

$$[\alpha] = [\alpha]_m \bar{l}\delta u/((\bar{l}\delta u)^2 + 1)^{1/2} \quad (18a)$$

or, using eq 16, to a function of the single parameter $\bar{l}E_h/RT$

$$[\alpha] = [\alpha]_m(\bar{l}E_h/RT)/((\bar{l}E_h/RT)^2 + 1)^{1/2} \quad (18b)$$

The result significantly demonstrates the polymeric amplification power of the expectedly tiny deuterium isotope effect. It shows that the specific optical rotation is determined by the energy difference per whole helical sequence rather than per monomer. Note that $\bar{l}\delta u$ depends on $1/RT$ exponentially through $\bar{l} = \exp(E_r/RT)$, and linearly through $\delta u = E_h/RT$ [in the more general case given in eq 10, through $\delta u = (\exp(E_h/RT) - \exp(-E_h/RT))/2$].

We conclude the presentation of case 2 of long polymers by comparing it with case 1. In both cases the specific optical rotation depends on the energy difference between whole sequences of M and P helices. These sequences are long because of the high energy cost of reversals, which introduces a cooperative behavior of the helical states: A P state cannot succeed an M state and vice versa, except if the two are separated by a reversal state of low probability. The long helical sequences serve as amplifiers of the small energy difference between P and M monomer units. However, in case 1 the helical sequence is that of the whole polymer, and its energy $NE_h$ is independent of temperature. In case 2, the length of the helical sequences, and therefore their energy difference $\bar{l}E_h$, vary exponentially with the inverse temperature $1/RT$.

**Case 3.** Here we use the partition function in its general form, applicable at all $N$ (see Appendix, eq A25 and A14):

$$Z_N = x_1^N(1 + v/w) + x_2^N(1 - v/w)$$

$$\text{where} \quad x_1 = \tfrac{1}{2}(u_M + u_P) + w \quad x_2 = \tfrac{1}{2}(u_M + u_P) - w \quad (19)$$

The quantities of interest, eq 4–6, are now derived by the partial derivatives of $Z_N$ of eq 19 with respect to $u_M$, $u_P$, and $v$.

Using the following table of partial derivatives

| $y$ | $\partial y/\partial u_M$ | $\partial y/\partial u_P$ | $\partial y/\partial v$ |
|---|---|---|---|
| $x_1$ | $(w + \delta u)/2w$ | $(w - \delta u)/2w$ | $v/w$ |
| $x_2$ | $(w - \delta u)/2w$ | $(w + \delta u)/2w$ | $-v/w$ |
| $w$ | $\delta u/2w$ | $-\delta u/2w$ | $v/w$ |
| $v/w$ | $-v\delta u/2w^3$ | $v\delta u/2w^3$ | $1/w - v^2/w^3$ |

one obtains

$$\partial Z_N/\partial u_M = [Nx_1^{N-1}(w + v)(w + \delta u) - x_1^N v\delta u/w + Nx_2^{N-1}(w - v)(w - \delta u) + x_2^N v\delta u/w]/2w^2 \quad (20a)$$

$$\partial Z_N/\partial u_P = [Nx_1^{N-1}(w + v)(w - \delta u) + x_1^N v\delta u/w + Nx_2^{N-1}(w - v)(w + \delta u) - x_2^N v\delta u/w]/2w^2 \quad (20b)$$

$$\partial Z_N/\partial v = [Nx_1^{N-1}(w + v)v + x_1^N(w - v^2/w) + Nx_2^{N-1}(w - v)v - x_2^N(w - v^2/w)]/w^2 \quad (20c)$$

The main quantity of interest, $[\alpha]$, is obtained from eq 6 and 20a,b, and by assuming $u_M \sim u_P \sim 1$ according to eq 12

$$[\alpha]/[\alpha]_m = \frac{Nx_1^{N-1}(w + v)\delta u - x_1^N v\delta u/w - Nx_2^{N-1}(w - v)\delta u + x_2^N v\delta u/w}{Nx_1^{N-1}(w + v)w + Nx_2^{N-1}(w - v)w} \quad (21)$$

To eliminate $x_1$ and $x_2$ from this equation we note that for $^1/_2(u_M + u_P) \sim 1$ and $w \ll 1$

$$x_2/x_1 \approx (1 - w)/(1 + w) = \exp[\ln(1 - w) - \ln(1 + w)] \approx \exp(-2w) \quad (22)$$

Therefore, to a good approximation,

$$[\alpha]/[\alpha]_m = (\delta u/w)\cdot(1 - v/(w + v)wN - \exp(-2wN)[(w - v)/(w + v) - v/(w + v)wN])/(1 + \exp(-2wN)(w - v)/(w + v)) \quad (23)$$

This equation is reduced to eq 17 of case 2 when $wN \gg 1$, because the correction terms in eq 23 vanish. It reduces to eq 8 of case 1 when $w \gg v$. In this case $\delta u/w$ approaches 1, and $[\alpha]$ is determined primarily by the correction terms in eq 23. Putting in the $v = 0$, $w = \delta u$, one obtains

$$[\alpha]/[\alpha]_m = [1 - \exp(-2\delta uN)]/[1 + \exp(-2\delta uN)] \quad (24)$$

which is equivalent to eq 8. The correction terms can be used to examine the ranges of validity of cases 1 and 2 for any set of values of $\delta u$ and $v$.

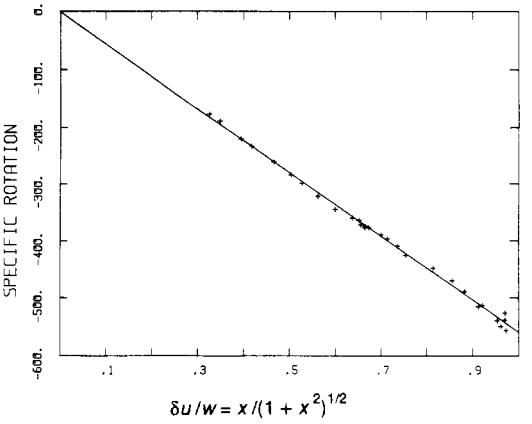


**Figure 1.** Plot of the experimental specific rotation ($[\alpha]$) in chloroform versus the dimensionless variable $x/(1 + x^2)^{1/2}$, where $x = \delta u/v$ (see text). Theoretical parameters: $[\alpha]_m = -559$; $E_r = 3874$ cal/mol; $E_h = 0.6854$ cal/mol. The straight line connects the points (0, 0) and (1, −559). Covariances: $[\alpha]_m E_r = 7.7$; $[\alpha]_m E_h = -7.9 \times 10^{-3}$; $E_r E_h = -0.31$.

**Comparison of Experiment and Theory.** As communicated recently,[15] the surprisingly high optical activity of anionically prepared poly((*R*)-1-deuterio-1-hexyl isocyanate) (**1**), which was shown by circular dichroism measurements to arise from an excess of one of the helical senses, is attended by a strong temperature dependence. This dependence is the connection to the theory developed in the current work to understand the forces responsible for the deuterium isotope effect observed.[15]

Fitting the experimentally determined change of specific rotation at the sodium D line, $[\alpha]$, with temperature, to the theory described above, requires determination of three independent variables: $\pm[\alpha]_m$, the D-line specific rotation of a sample homogeneous in helical sense; $E_r$, the energy per mole of a monomer unit in the helix reversal state; and $2E_h$, the energy difference per mole between the right-handed (P) and left-handed (M) helical monomer units. We examined the fit of cases 1, 2, and 3 of the theory to the experimental change of $[\alpha]$ with temperature over the range of +60 to −30 °C in dilute solutions of poly((*R*)-1-deuterio-*n*-hexyl isocyanate) **1** of $N = 6800$ ($M_w/M_n \sim 1.3$)[15] in chloroform or hexane. First, fitting to case 1 was attempted by least-square procedures (see below) and failed totally. The attempted fit showed the experimental dependence of $[\alpha]$ on temperature to be of too large a slope for case 1 and demonstrated that the necessary prerequisite assumption of no helix reversals for this polyisocyanate (**1**) of $M_w = 870\,000$[15] was unwarranted.

The experimental specific rotation values were fit to the theoretical function of case 2, given in eq 18 as a function of the single variable, $x = \bar{l}\delta u = \delta u/v$. A modification of the Levenberg–Marquardt algorithm[18] was used to minimize the sum of the squares of the differences between the calculated theoretical $[\alpha]$ and the experimental $[\alpha]$. The least-squares procedure used analytical derivatives of the theoretical $[\alpha]$ with respect to each of the parameters. The experimental data were found to fit case 2 of the theory for reasonable values of the three independent variables. The results are expressed in Figures 1 and 2 as a plot of the measured specific rotation versus the dimensionless theoretical parameter $x/(1 + x^2)^{1/2}$ described above. Straight lines are obtained by using data for both chloroform and hexane so-

(18) More, J. J. . *The Levenberg–Marquardt Algorithm. Implementation and Theory, Numerical Analysis*; Watson, G. A., Ed.; Lecture Notes in Mathematics 630; Springer-Verlag: New York, 1977.

**Table I.** Parameters Determined from Comparison of the Experimental [α] vs Temperature to the Cases 3 and 2 Theories[a]

| case | solvent | $[\alpha]_{max}$ | $2E_h$[a] | $E_r$[a] | $\bar{l}$[b] 273 K | $\bar{l}$[b] 300 K | $\bar{l}_M/\bar{l}_P$[c] 273 K | $\bar{l}_M/\bar{l}_P$[c] 300 K |
|---|---|---|---|---|---|---|---|---|
| 3 | $CHCl_3$ | −581 ± 3° | 0.40 ± 0.08 | 4707 ± 54 | 5546 | 2553 | 20 | 5 |
| | hexane | −590 ± 1° | 0.76 ± 0.10 | 4426 ± 80 | 3315 | 1598 | 25 | 6 |
| 2 | $CHCl_3$ | −559 ± 0.6 | 1.36 ± 0.04 | 3874 ± 17 | 1206 | 637 | | |
| | hexane | −576 ± 0.7 | 1.38 ± 0.04 | 4094 ± 22 | 1805 | 919 | | |

[a] See text for explanation of terms. The ± variability is 1 standard deviation from the fit to the particular theoretical case indicated. Energy units for $2E_h$ and $E_r$ are calories/mole-monomer unit. [b] Geometric mean of the number of monomer units between helix reversals for poly(*n*-hexyl isocyanate) at 300 and 273 K. [c] Ratio of average length of left-handed ($\bar{l}_M$) and right-handed ($\bar{l}_P$) helical sequences in poly(*R*)-1-deutero-1-hexyl isocyanate) at 300 and at 273 K. These numbers, calculated from the parameters, are the same for cases 2 and 3.

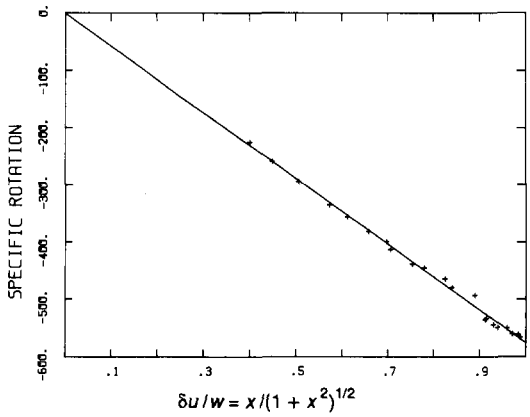


**Figure 2.** Plot of the experimental specific rotation in hexane ([α]) versus the case 2 theoretical parameter as in Figure 1. Theoretical parameters: $[\alpha]_m = -576$; $E_r = 4094$ cal/mol; $E_h = 0.6905$ cal/mol. Covariances: $[\alpha]_m E_r = 11$; $[\alpha]_m E_h = -1.0 \times 10^{-2}$; $E_r E_h = -0.48$.

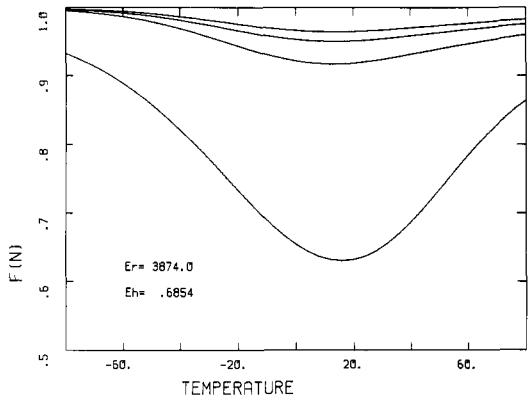


**Figure 3.** Plot of the correction factor following $\delta u/w$ in eq 23 as a function of temperature for the values of $E_h$ and $E_r$, derived from the case 2 theory, for chloroform. Each line in descending order corresponds to the value of $N$ equals 7000, 5000, 3000, and 1000.

lutions for the optimal values of the independent variables noted in Figures 1 and 2.

Next, we examined the effect of the correction factor for the general case 3 on the calculated values of [α], using the optimized values $E_r$ and $E_h$ obtained from the case 2 fit discussed above. This factor, which follows ($\delta u/w$) in eq 23, is the correction factor that takes account of the situation where the infinite chain assumption of case 2 may be inadequate. In Figures 3 and 4 this correction factor is plotted for several values of $N$ over the experimental temperature range for the data in chloroform and hexane, respectively. As can be judged from Figures 3 and 4, the difference between the correction factor and unity is small but finite over the experimental range of our measurements ($N$ = 6800). For this reason we applied the same least-squares procedure, described above,[18] for the fit of the experimental data to the theoretical expression, eq 23, for case 3. The optimal values for $[\alpha]_m$, $E_h$, and $E_r$ from this fit differ from those of the case 2 fit, while the merit of the two cases, as judged by the standard deviations is similar (Table I). This is a puzzling situation. The

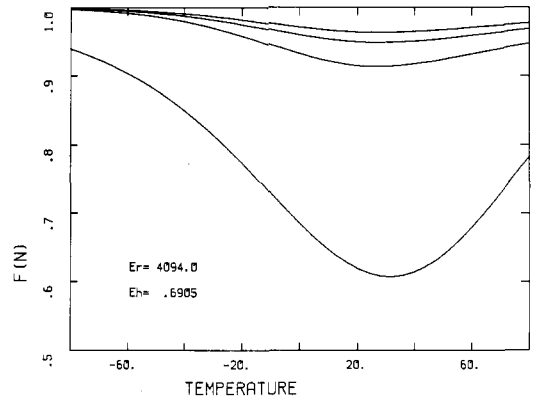


**Figure 4.** Same as for Figure 3 for the parameters for hexane.

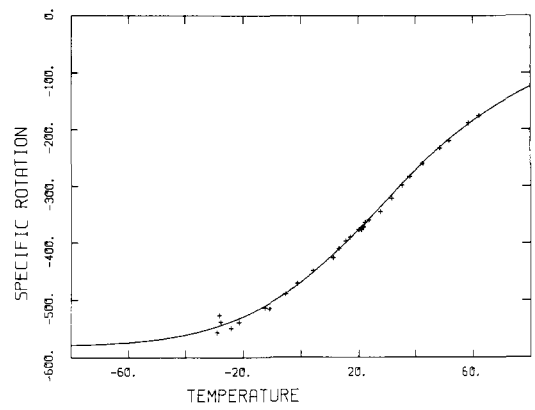


**Figure 5.** Plot of the specific rotation ([α]) versus temperature for the experimental data for chloroform (points) and the predicted relationship for the case 3 theory from eq 23 (contiuous line) for the theoretical parameters: $[\alpha]_m = -581$, $E_r = 4707$ cal/mol; $E_h = 0.20$ cal/mol. Covariances: $[\alpha]_m E_r = -97$; $[\alpha]_m E_h = 2.9 \times 10^{-2}$; $E_r E_h = -0.56$.

differences between cases 2 and 3 (Table I) viewed against the smallness of the $N$ dependence for the correction factor as observed in Figures 3 and 4 for $N$ values from 7000 to 3000 (which are well beyond the estimated polydispersity of **1**[15] are inexplicably large. Work is underway to overcome this by preparing a wide variety of molecular weights of **1** and subjecting these materials to the analysis discussed above. The significant covariance between the pairs of parameters, $[\alpha]_m$, $E_h$, and $E_r$, reported in the footnotes to Figures 1, 2, 5, and 6 quantify the fitting difficulties. Figures 5 and 6 show the predicted curves, in chloroform and hexane respectively, for the specific rotation versus temperature for the case 3 general theory, using these variables reported in Table I, matched against the experimental data.

## Discussion

The comparison of the theory and the experimental data shown above (Figures 1–6, Table I) constitutes an independent verification of the conclusions of the literature[5-11] on the solution properties of poly(*n*-alkyl isocyanates) as adopting wormlike helical conformations interrupted by occasional helix reversals. It justifies in quantitative detail the cooperative phenomenon invoked[15] to explain the surprising effect of asymmetric deuterium substitution

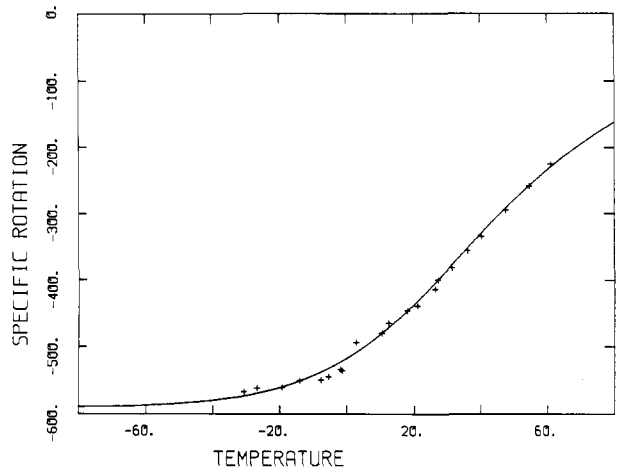


**Figure 6.** Plot of the specific rotation ([α]) versus temperature for the experimental data for hexane (points) and the predicted relationship for the case 3 theory from eq 23 (continuous line) for the theoretical parameters: $[\alpha]_m = -590$, $E_r = 4426$ cal/mol; $E_h = 0.38$ cal/mol. Covariances: $[\alpha]_m E_r = -58$; $[\alpha]_m E_r = 3.3 \times 10^{-2}$; $E_r E_h = -4.2$.

on the relative helical sense stability.

As seen in Table I, the correlation of the theoretical and experimental effort has allowed the approximate determination of a tiny energy difference between the helical senses $2E_h$, which would be extremely difficult to distinguish in the absence of the cooperative effect.

The helical sense in excess in poly((*R*)-1-deuterio-*n*-hexyl isocyanate) (**1**) could not be assigned directly. However, in poly((*R*)-2,6-dimethyl-*n*-heptyl isocyanate)[15] where the diastereomeric interactions between the stereogenic center and the helical backbone are more easily defined, preliminary force field calculations[19] show a clear preference for the M helix. Since the circular dichroism spectra of the two optically active polyisocyanates are of the same sign and shape[15] we may, on this basis, assign the excess helical sense in the deuterated polyisocyanate as M.

Models that are constructed based on the helix sense information discussed above cannot be related to a structural source for the deuterium isotope effect, an outcome that would be reasonably expected for a helical sense difference of only ~1 cal/mol per deuterium. The source of the energy difference could be either some interactions of D or H with neighboring atoms or vibrational frequency shifts (or both).[20] It is practically impossible by methods now available to trace these sources or to find a theoretical basis to calculate this tiny difference in such a complex system.

This difficulty can be expressed quantitatively by the realization that the energy one might seek to interpret, if one were to assign it to a single frequency shift, translates to only a difference of ~3 $cm^{-1}$ in the expected frequencies[20] of the C–D infrared bands for the C-1 deuterium in **1** with a left- or a right-handed helical backbone. This is far below the corresponding threshold of resolution in the cast film infrared spectrum of **1**[21] where we can be assured by the specific rotation that the deuterium motions of both diastereotopic relationships are present.

The dilemma faced above, of knowledge of an energy parameter that is too small to be understood by available theory, can be amplified to a still higher level. Measurements of optical rotations far smaller than measured here (see Figures 5 and 6), and in addition nearer to the wavelengths of the responsible chromophores (250 nm and lower wavelength)[22] based on expectations of how the rotation of the plane of polarized light changes for the D line into the maxima of the Cotton Effect,[23] especially for an inherently dissymmetric chromophore,[24] could be expected to lower the detectable limit by at least 3 orders of magnitude. Such extremely small per residue energies favoring one helical sense (i.e., <0.001 cal/mol per residue) suggest looking at chiral perturbations, in high molecular weight poly(*n*-alkyl isocyanates), which are far smaller than the deuterium stereogencity studied in **1**. In this way the poly(*n*-alkyl isocyanates), or other systems with analogous properties, via the amplification arising from cooperativity, offer the opportunity to see the spectroscopic consequences and to measure the energetic parameters of chiral forrces so tiny as to be generally undetectable.[25]

The parameter $E_r$ (Table I), which is the energy of a helix sense reversal relative to the helical state, is related to the long-standing question of the responsible structural feature for the transition from rod- to worm- to coillike properties as molecular weight increases in poly(*n*-alkyl isocyanates). The change of radius of gyration,[5] viscosity,[6] and dipole moment[7] with degree of polymerization, $N$, is characteristic of a rod at molecular weights corresponding to $N$ less than ~1000 with scaling characteristics of a random coil at $N$ in excess of 10000. In the intermediate region the polyisocyanates are well described by the Kratky–Porod wormlike model.[5-10] The details of this transition from rod to coil are surprisingly solvent dependent, which can be quantitatively expressed by the persistence lengths, which vary from ~200 to ~400 Å in polar and nonpolar solvents, respectively.[6] This conformational transition from the extremes of rod to coil with increasing molecular weight, i.e., axial dimension, which is a signature of stiff polymers,[2,3] is exactly analogous to the familiar behavior of a macroscopic object with a large ratio of axial to lateral dimension, e.g., imagine a steel rod as its length increases. Although in poly(*n*-alkyl isocyanates) Cook[9] has shown that small local torsional motions and angle deformations are adequate to account for the experimental observations, the contribution of helix reversals to the polymer shape is an open questions.[10] The specific change in chain direction associated with such an interruption would designate the polymer as a broken rod or worm[2] and polyisocyanates, along with DNA, have been the subject of theoretical investigations to predict the means to detect such behavior.[10] This work[10] shows that relative contribution of torsional and angular local movement and of specific breaks to the persistence lengths of stiff polymers can be evaluated by eq 25, where $a$ and

$$\frac{1}{a} = \frac{1}{a_w} + \frac{1 - \cos\theta}{b} \qquad (25)$$

$a_w$ are the experimental persistence length and the portion of this length due to only local motions, respectively.[10] The contour distance between specific breaks, i.e., helix reversals, and the angular direction at the break are $b$ and $\theta$, respectively. We now have the means to evaluate the equation since $E_r$, via eq 2, yields the number of monomer units between breaks (Table I), which when multiplied by the monomer projection length, known[8,26] to be near to 2 Å, yields $b$. Evaluation[27] of helical models indicates

(19) Collaborative work in progress at the Polytechnic University and at the Weizmann Institute.

(20) Hydrogen deuterium isotope effects may be categorized as kinetic or structural. For leading references to the former literature see: Green, M. M.; Boyle, B. A.; Vairamani, M.; Mukhopadhyay, T.; Saunders, W. H., Jr.; Bowen, P.; Allinger, N. L. *J. Am. Chem. Soc.* **1986**, *108*, 2381. There has been much recent interest in the latter category. See: Anet, F. A. L.; Kopelevich, M. *J. Am. Chem. Soc.* **1986**, *108*, 1355; *Ibid.* 2109. Anet, F. A. L.; Kopelevich, M. *J. Chem. Soc., Chem. Commun.* **1987**, 595. Servis, K. L.; Domenick, R. L.; Forsyth, D. A.; Pan, Yi. *J. Am. Chem. Soc.* **1987**, *109*, 7263. Forsyth, D. A.; Botkin, J. H.; Puckace, J. S.; Servis, K. L.; Domenick, R. L. *Ibid.* 7270. Forsyth, D. A.; Hanley, J. A. *Ibid.* 7930. For a review of the earlier literature see: Melander, L.; Saunders, W. H., Jr. *Reaction Rates of Isotopic Molecules*; Wiley-Interscience: New York, 1980; pp 189–201.

(21) See the Experimental Section.

(22) Milstien, J. B.; Charney, E. *Macromolecules* **1969**, *2*, 678. Troxell, T. C.; Scheraga, H. A. *Ibid.* **1969**, *2*, 678.

(23) Djerassi, C. *Optical Rotatory Dispersion*; McGraw Hill: New York, 1960. For a recent work in a closely related area see: Harada, N.; Nakanishi, K. *Circular Dichroic Spectroscopy*; University Science Books: Mill Valley, CA 1983.

(24) A polyisocyanate fits this definition. See: Mislow, K. *Introduction to Stereochemistry*; Benjamin: Reading, MA, 1965; pp 65–66.

(25) See: Solladie, G.; Gottarelli, G. *Tetrahedron* **1987**, *43*, 1425, and references therein. See also: Lightner, D. A.; McDonagh, A. F.; Wijekoon, W. M. D.; Reisinger, M. *Tetrahedron Lett.* **1988**, *29*, 3507, and previous references in this area. Mason, S. F. *Proc. Chem. Soc., London* **1964**, 119.

(26) Shmueli, K.; Traub, W.; Rosenheck, K. *J. Polym. Sci., Part A-2* **1969**, *7*, 515.

$\theta$ to be near to 35°. Under these conditions, and using the limiting experimental values of 200 and 400 Å in polar and nonpolar solvents, respectively,[6] for $a$, one calculates $a_w$ to be nearly equal to $a$ from the measured persistence lengths in these solvent classes for the range of values of $E_r$ found in Table I.

Thus, we can conclude that the overall chain dimensions of poly(*n*-hexyl isocyanate), and reasonably other poly(*n*-alkyl isocyanates), in solution depend largely upon the magnitude of torsional and angular oscillations and not on the occurrence of helix reversals. It also must follow that the long sought answer[5,6] to the unusual solvent dependence of poly(*n*-alkyl isocyanate) dimension is that the cause arises from larger torsional or angular motions,[9] or both, in the case of more polar solvents.[5,28] These conclusions suggest that nuclear magnetic resonance relaxation time measurements of the poly(*n*-alkyl isocyanates) would be well directed to understanding the unit source of global dimension in these polymers.[29]

## Experimental Procedures

**Instrument Procedures.** For the synthetic procedures leading to poly((*R*)-1-deuterio-1-hexyl isocyanate) (**1**), proton and $^{13}C$ NMR spectra were taken, respectively, on a Varian EM-390 and a JEOL-FX-90Q spectrometer and infrared spectra on a Schimatzu IR 435 and a Digilab FTS-60 FTIR spectrometer. Optical rotations were measured both for intermediates in the synthesis and for the temperature dependence of the $[\alpha]_D$ of **1** on a Perkin-Elmer 141 polarimeter. The temperature-dependent measurements on **1** were carried out in chloroform and in hexane at concentrations of $8 \times 10^{-4}$ g/mL. The temperature dependence was found to be independent of concentration within a 100-fold dilution. A jacketed 1-dm cell using a Haake constant temperature bath filled with 2-propanol/ethanol with auxiliary coiling provided by a Neslab Cryo Cool CC-60 immersion coil cooler was used. Gaseous nitrogen from liquid nitrogen blowoff was impinged directly on the polarimeter cell windows at a temperature and rate both to adjust the cell window to within 1 °C of the thermostating fluid and to avoid condensation. The sample section of the polarimeter was maintained in a dry nitrogen atmosphere. The cell window temperature was measured with a contact thermocouple, Type T-SLE manufactured by Omega Engineering, connected to a thermocouple thermometer Model 450 ATT with a total precision of ±0.5 °C. The thermostating fluid temperature was measured inside the cell jacket with the same thermocouple. All deuterated intermediates were shown to be identical with nonisotopically substituted standards by gas chromatography on a Perkin-Elmer 990 FID-GC using a 20-ft. 3% SE-30 column. Intrinsic viscosity was measured on a single-bulb Cannon-Ubberlohde type viscometer uncorrected for shear-rate dependence.

**Synthetic Procedures.** Ethyl hexanoate (16 g, 0.11 mol) was reduced with lithium aluminum deuteride (3.5 g, 0.08 mol) at 0 °C in dry ethyl ether to yield 9.5 g (83%) of 1,1-dideuteriohexanol. A 4.3-g (0.04-mol) aliquot of the latter alcohol was treated with 19 g (0.088 mol) of pyridinium chlorochromate, synthesized following the literature,[30] in dichloromethane (220 mL) at 40 °C for 2.5 h to yield 1-deuteriohexanal in 50% yield.

D-(+)glucose (500 g) was dissolved in 2500 mL of deionized water and equilibrated at 36.5 °C. Over a period of 24 h, 800 g of Budweiser baker's yeast, 400 g more of glucose, and 10 g (in two batches) of 1-deuteriohexanal washed in with 3 mL of ethanol were added and fermentation commenced as evidenced by gas evolution. The flask was sealed except for a gas outlet through a water bubbler, i.e., anaerobic conditions. The fermentation was continued for 40 h more. Workup involved addition of 500 g of NaCl followed by steam distillation and ether extraction, yielding after distillation 7.7 g (75% yield) of (*S*)-1-deuteriohexanol, $[\alpha]^{22.5}_D$ +0.31° (neat, 1 dm). The configuration was assigned in analogy to other aldehyde reductions.[31]

The (*S*)-deuterio-1-hexanol was converted to the brosylate following the literature.[32] This substance, formed in high yield, was used without purification. A 27.5-g portion of this brosylate was dissolved in 41 mL of *N*,*N*-dimethylformamide; to this was added 22.6 g (0.35 mol) of sodium azide dissolved in 70 mL of water to which was added 1.8 g of Aliquot 336 (Aldrich Chemical Co.). After 45 h at 80 °C, water was added to dissolve the salts and the (*R*)-1-deuterio-1-azidohexane (IR, 2090 $cm^{-1}$) was obtained by extraction with ether [yield 77%, based on (*S*)-deuteriohexanol (7.1 g)]. Without further characterization, the azide was reduced with 2.1 g (0.055 mol) of lithium aluminum hydride in refluxing ether to yield (*R*)-1-deuterio-1-aminohexane (3.4 g, yield 61%): $[\alpha]^{22}_D$ −0.04° (neat, 1 dm); IR, weak doublet at 2155 and 2110 $cm^{-1}$ for deuterium as described also for 1-deuterio-1-aminobutane.[33] A $^{13}C$ NMR spectrum of the hydrochloride salt in $D_2O$ exactly fit the spectrum of standard 1-aminohexane hydrochloride with the exception that the lowest field line at 37.7 ppm was split into a triplet of equal intensities.

(*R*)-1-Deuterio-1-aminohexane (HCl) [2.22 g (0.016 mol)] described above was mixed with 15 mL of tetralin (washed with sulfuric acid and distilled from sodium)[34] under anhydrous conditions with stirring and with an argon bubbler, which was switched to phosgene at 130 °C. The temperature was rapidly raised to 170 °C with continuous bubbling of phosgene for 2 h. The reaction was monitored by IR spectroscopy at 2265 $cm^{-1}$ after complete dissolution of the amine hydrochloride. After purging with argon and lowering of the temperature, the IR spectrum showed no phosgene (1805 $cm^{-1}$ absent). The (*R*)-1-deuterio-1-hexyl isocyanate was obtained by several distillations through Vigreux columns (ca. 10–15 mm, ca. 60 °C) (0.7 g, 37% yield). Gas chromatography showed this material to be identical with standard hexyl isocyanate. The optical rotation of this material was not taken because there was too small an amount to fill the polarimeter cell and it was too precious to dilute. A subsequent preparation yielded enough material to measure as $[\alpha]^{25}_D$ + 0.65° (neat, 1 dm).

**Poly((*R*)-1-deuterio-1-hexyl Isocyanate).** Following the literature,[4] the entire sample (0.7 g), directly from the distillation, was dissolved in 4 mL of dimethylformamide. The latter solvent was distilled at 43–44 °C from $P_2O_5$ with a pot temperature below 60 °C under 8–10 mm of argon. No grease was used and only the middle distilled cut was used. Dry syringes through septa were used for all transfers. The initiator was prepared from 0.64% wt/vol of dry NaCN in the just-described DMF. Three drops of the initiator solution were added quickly with stirring to the monomer solution at −58 °C in a serum capped side-arm test tube under dry argon. The solution became almost immediately opaque and gelled. After 30 min, 10 mL of −50 °C methanol was added and the mass was triturated with a spatula. This was scooped out and vacuum filtered on Whatman No. 1 filter paper to yield a white fibrous solid. This material was dissolved in 150 mL of chloroform, scrubbed previously with $CaCO_3$ and dropped into 150 mL of rapidly stirred methanol. After filtering and drying, there was obtained 0.52 g (74% yield) of a white fibrous solid. This material had UV (350–200 nm) and IR (4000–1400 $cm^{-1}$) spectra, except for the C–D stretch at 2221 $cm^{-1}$, identical with standard[4] poly(*n*-hexyl isocyanate): UV (hexane, 22 °C) 252 nm ($4.66 \times 10^3$ L/mol·cm), 204 nm ($3.35 \times 10^3$ L/mol·cm); IR (film cast from $CHCl_3$) carbonyl stretch, 1697.4 $cm^{-1}$; optical rotation, $[\alpha]^{25}_D$ −367° (*c* 0.08, $CHCl_3$).

**Acknowledgment.** The work in Brooklyn was supported by the National Science Foundation (Grant CHE-8615872) and by the donors of the Petroleum Research Fund, administered by the American Chemical Society. We are grateful for this support. We also thank Professor D. A. Forsyth, Northeastern University, and Dr. R. Cook, Lawrence Livermore National Laboratory, for helpful discussions. We are also grateful to Professor H. Morawetz of the Polytechnic University for introducing M.M.G. and S.L. and to Frank T. Green for his cooperation.

## Appendix

The partition function $Z_N$ for chiral polyisocyanates of length $N$ depends on $E_r$, $E_h$, and $T$ through $u_M$, $u_P$, and $v$ (eq 3). $Z_N$ is derived here by the sequence generating functions method for partition functions of linear polymers. The method was obtained first for the case of infinitely long polymers[16] and then extended

(27) This corresponds to torsion angles at the helix reversal of 40, 160; −40 200; 40, 200 as defined in ref 8. Unpublished calculation of Dr. R. Cook, Lawrence Livermore National Laboratory.

(28) Collaborative work at the Polytechnic University, Lawrence Livermore Laboratories (Dr. R. Cook), and at IBM (Dr. R. D. Johnson, Almaden) is in progress to define this interaction.

(29) Bovey, F. A. *Nuclear Magnetic Resonance Spectroscopy*, 2nd ed.; Academic Press: New York, 1988.

(30) Corey, E. J.; Suggs, J. W. *Tetrahedron Lett.* **1975**, *31*, 2647. We made numerous attempts, without success, to follow a new procedure for the synthesis of hexanal. See: Cha, J. S., Kwon, S. S. *J. Org. Chem.* **1987**, *52*, 5486.

(31) For leading references see: Arigoni, D.; Eliel, E. L. *Top. Sterechem.* **1969**, *4*, 127. See pp 164–166 therein.

(32) Kabalka, G. W.; Varma, M.; Varma, R. S.; Srivastava, P. C.; Knapp, F. F., Jr. *J. Org. Chem.* **1986**, *51*, 2386.

(33) Streitwieser, A., Jr.; Schaeffer, W. D. *J. Am. Chem. Soc.* **1956**, *78*, 5597.

(34) Perrin, D. D.; Armarego, W. L. F.; Perrin, D. R. *Purification of Laboratory Chemicals*; Pergamon Press: New York, 1980.

for the general case of any $N$.[17] It is simpler and more versatile than the matrix method, which is, nevertheless, equally applicable if it is adapted to the general case of any $N$.[35]

A microscopic state of a polyisocyanate chain is specified by the number of the consecutively alternating M and P helical sequences, and by their respective lengths. A chain may start, and also end, with either M or P sequences. Consequently, the number of alternating sequences may be even, $2s$, or odd, $2s + 1$, with $s \leq N/2$. The lengths of the sequences are denoted by $i_\sigma$ and $j_\sigma$ for M and P helical sequences, respectively. Symbolically, then, a microscopic state $\underline{\text{ms}}$ is

$$\underline{\text{ms}} = i_0, j_1, i_2, \cdots, j_\sigma, i_\sigma, \cdots, j_s, i_s;\ s = 0, 1, \cdots, N/2 \qquad \text{(A1a)}$$

when the chain starts and ends with a M sequence. It is similarly

$$\underline{\text{ms}} = j_0, i_1, j_1, \cdots, i_\sigma, j_\sigma, \cdots, i_s, j_s \qquad \text{(A1b)}$$

in the opposite case.

All sequences except the last must contain at least one monomer unit. The last sequence in (A1a), $i_s$, vanishes when the chain ends with $j_s$, and similarly for $j_s$ in (A1b). The range of variability of the $i$'s and $j$'s is restricted by the requirement that their sum should be equal to the length of the polymer, i.e.

$$\sum_{\sigma=0}^{s} (i_\sigma + j_\sigma) = N,\ s \leq N/2 \qquad \text{(A2)}$$

Every two consecutive sequences are separated by a transition monomer unit, which is designated as the first unit of the following sequence. Based on the definition of $u_M$, $u_P$, and $v$, the statistical weights of M helical sequences are

$$u_{i_0} = u_M^{i} \qquad u_{i_\sigma} = v u_M^{i-1} \qquad 1 \leq \sigma \leq s \qquad \text{(A3a)}$$

Similarly for P sequences

$$u_{j_0} = u_P^{j} \qquad u_{j_\sigma} = v u_P^{j-1} \qquad \text{(A3b)}$$

The statistical weight $\underline{w}(\underline{\text{ms}})$ of a microscopic state of the polymer chain is a product of the statistical weights of its sequences as defined above.

$$\underline{w(\text{ms})} = \prod_{\sigma=0}^{s} u_{i_\sigma} u_{j_\sigma} = u_M^{m_M} u_P^{m_P} v^{m_v} \qquad \text{(A4)}$$

Alternatively, it may be presented as the product of the statistical weights of the monomers of helicity M, of helicity P and of reversal conformations whose numbers for a given microscopic state are here denoted as $m_M$, $m_P$, $m_v$, respectively. The two alternative representations of $\underline{w}(\underline{\text{ms}})$ shown in (A4) are precisely equivalent. The second representation is useful in order to obtain the corresponding averages $n_M$, $n_P$, $n_v$ according to eq 4. The partition function, $Z_N$, is the sum over the whole set {ms}, subject to the restriction imposed by eq A2

$$Z_N = \sum_{\{\underline{\text{ms}}\}} \underline{w(\text{ms})} \qquad \text{(A5)}$$

(or the equivalent restriction, $m_M + m_P + m_v = N$). In the sequence generating functions method the partition functions $Z_N$ are derived through the "polymer generating function" $\Gamma(x)$; $\Gamma(x)$ is derived from the "sequence generating functions", in our case $U_M(x)$ and $U_p(x)$ and $U_{o,M}(x)$ and $U_{o,P}(x)$ (see below); the sequence generating functions are obtained from the statistical weights attributed to the microscopic states; finally, $Z_N$ is derived as a function of these statistical weights. The application of these steps to polyisocyanates follows.

$\Gamma(x)$ is a power series in $1/x$ with $Z_N$ as coefficients

$$\Gamma(x) = \sum_{N=1}^{\infty} Z_N x^{-N} = \sum_{N=1}^{\infty} \sum_{\{\underline{\text{ms}}\}} \underline{w(\text{ms})} x^{-\Sigma(i_\sigma + j_\sigma)} \qquad \text{(A6)}$$

$U_M(x)$ and $U_P(x)$ are defined for all sequences except the first sequence of a chain by

$$U_M(x) = \sum_{i=1}^{\infty} u_i x^{-i} = \sum v u_M^{i-1} x^{-i} = v/(x - U_M)$$

$$U_P(x) = \sum u_j x^{-j} = v/(x - U_P) \qquad \text{(A7)}$$

The sequence generating functions for the beginning of a chain are

$$U_{0,M}(x) = \sum_{i=0}^{\infty} u_i^{i} x^{-i} = x/(x - u_M) = (x/v) U_M(x)$$

and similarly $$U_{o,P}(x) = (x/v) U_P(x) \qquad \text{(A8)}$$

Note that the summation starts from $i = 0$ rather than $i = 1$. This allows for the possibility, which is rare but is not forbidden, that the first unit of the chain acquires a "reversal conformation". Since the same possibility is allowed for the last unit of the chain according to eq A7 the enumeration of states is thus made complete (which a propos has the advantage of maximum mathematical simplicity). The series $\Gamma(x)$ converges when $x$ is sufficiently large, so that $Z_N x^{-N} < 1$ for all large values of $N$. The series $U_M(x)$ and $U_P(x)$ converge if $\Gamma(x)$ converges, because they are contained in $\Gamma(x)$. The crux of the sequence generating functions method is that it expresses $\Gamma(x)$ in terms of the sequence generating functions. The detailed mathematical derivation of such a relation[16] rests on the following simple consideration: The restrictions imposed by eq A2 on enumerating $\underline{\text{ms}}$ are waived when summing over all $N$, since all conceivable chain lengths and number of alternations are included in $\Gamma(x)$. Considering that a polymer chain starts and ends with either M or P sequences, $\Gamma(x)$ is given rigorously by

$$\Gamma(x) = (x/v) \left[U_M \sum_{s=0}^{\infty} (U_P U_M)^s + U_P \sum_{s=0}^{\infty} (U_M U_P)^s + \sum_{s=1}^{\infty} (U_M U_P)^s + \sum_{s=1}^{\infty} (U_P U_M)^s\right] \qquad \text{(A9)}$$

While mathematical details are given in ref 16, the reader may verify by inspection that $\Gamma(x)$, as presented in the four terms in eq A9, scans precisely all possible conformations of all lengths of polymers. It includes chains from single monomer units to polymers of any length, and for each chain it allows for any monomer unit to obtain any of the three possible states: M helix; P helix; or reversals (V). Thus $\Gamma(x)$ of eq A9 is necessarily equal to $\Gamma(x)$ as defined in eq A6. For all $x$ for which the sums over $s$ converge, $\Gamma(x)$ is

$$\Gamma(x) = (x/v)(U_M + U_P + 2U_M U_P)/(1 - U_M U_P) \qquad \text{(A10)}$$

We now insert eq A7 and A8 into eq A10 and obtain $\Gamma(x)$ as a ratio of two polynomials, $x f(x)$ and $g(x)$:

$$\Gamma(x) = x f(x)/g(x) \qquad \text{(A11)}$$

where

$$f(x) = 2x - u_M - u_P + 2v \qquad \text{(A12)}$$

and

$$g(x) = (x - u_M)(x - u_P) - v^2 \qquad \text{(A13)}$$

It is worth noting that $f(x)$, representing the numerator in eq A10, depends on the detailed consideration of how the chain starts and ends, while $g(x)$, representing the denominator of that equation, depends on the bulk of alternating sequences.

Thus in the limit of $N \to \infty$ (case 2 in the text), only properties of $g(x)$ count. $g(x)$ is a quadratic polynomial, with roots

$$x_1 = \tfrac{1}{2}(u_M + u_P) + w \qquad x_2 = \tfrac{1}{2}(u_M + u_P) - w \qquad \text{(A14)}$$

where

$$w^2 = \delta u^2 + v^2 \qquad \delta u = (u_M - u_P)/2 \qquad \text{(A15)}$$

The criterion of convergence of $\Gamma(x)$, $Z_N x^{-N} < 1$, is fulfilled for all values of $x$ that are larger than $x_1$, the largest root of $g(x)$. It approaches the point of divergence as $x$ decreases toward $x_1$. Therefore $Z_N$ for all sufficiently large values of $N$ is given by

(35) Lifson, S.; Roig, A. *J. Chem. Phys.* **1961**, *34*, 1963.

$$Z_N = x_1^N \quad \text{(A16)}$$

In order to extract all the information contained in $\Gamma(x)$ about the polymer's properties at any value of $N$ (case 3 in the text), we must also make use of $f(x)$, as well as of $g(x)$'s second root, $x_2$. This is obtained[17] by developing $f(x)/g(x)$ in a power series in $1/x$, with coefficients that are functions $x_1$, $x_2$, $f(x_1)$, and $f(x_2)$, as follows: (1) First, $g(x)$ is factorized as

$$g(x) = (x - x_1)(x - x_2) \quad \text{(A17)}$$

and $f(x)/g(x)$ is transformed, by the method of "partial fractions", to

$$\frac{f(x)}{g(x)} = \frac{C_1(x - x_2) + C_2(x - x_1)}{(x - x_1)(x - x_2)} = \frac{C_1}{x - x_1} + \frac{C_2}{x - x_2} \quad \text{(A18)}$$

For this transformation to be fulfilled, $C_1$ and $C_2$ must satisfy the equation

$$f(x) = C_1(x - x_2) + C_2(x - x_1) \quad \text{(A19)}$$

therefore

$$C_1 = f(x_1)/(x_1 - x_2) \qquad C_2 = f(x_2)/(x_2 - x_1) \quad \text{(A20)}$$

(2) Next, $1/(x - x_1)$ and $1/(x - x_2)$ are developed in the power series

$$1/(x - x_1) = (1/x)\sum_{N=0}^{\infty}(x_1/x)^N$$
$$1/(x - x_2) = (1/x)\sum_{N=0}^{\infty}(x_2/x)^N \quad \text{(A21)}$$

(3) Finally, eq A18-A21 are put together into eq A11 for $\Gamma(x)$. The result is

$$\Gamma(x) = \sum_{N=0}^{\infty}[x_1^N f(x)/(x_1 - x_2) + x_2^N f(x_2)/(x_2 - x_1)]x^{-N} \quad \text{(A22)}$$

Both eq A22 and A6 express $\Gamma(x)$ as the same power series in $x^{-N}$. Therefore

$$Z_N = x_1^N f(x_1)/(x_1 - x_2) + x_2^N f(x_2)/(x_2 - x_1) \quad \text{(A23)}$$

holds for any value of $N$. In view of eq A12 and A14

$$f(x_1)/(x_1 - x_2) = (w + v)/w, f(x_2)/(x_2 - x_1) = (-w + v)/(-w) \quad \text{(A24)}$$

therefore

$$Z_N = x_1^N(1 + v/w) + x_2^N(1 - v/w) \quad \text{(A25)}$$

It may be verified by inspection that eq A25 is precisely valid for all $N$, from monomers and dimers to infinite polymers.

**Registry No.** Ethyl hexanoate, 123-66-0; 1,1-dideuteriohexanol, 52598-04-6; 1-deuteriohexanal, 55320-52-0; (*S*)-1-deuteriohexanol, 91525-95-0; (*R*)-1-deuterio-1-azidohexanal, 121987-97-1; (*R*)-1-deuterio-1-aminohexanal, 121987-98-2; (*R*)-1-deuterio-1-hexyl isocyanate, 114942-16-4; (*R*)-1-deuterio-1-hexyl isocyanate (homopolymer), 114507-38-9; (*R*)-1-deuterio-1-hexyl isocyanate (SRU), 114507-37-8.

# A Laser Flash Photolysis Study of Photodehydroxylation Phenomena of 9-Phenylxanthen-9-ol and Photobehavior of Related Intermediates. Enhanced Electrophilicity of 9-Phenylxanthenium Cation Singlet[1]

**Robert E. Minto[2a] and Paritosh K. Das*[,2b]**

*Contribution from the Radiation Laboratory, University of Notre Dame, Notre Dame, Indiana 46556.* *Received April 6, 1989*

**Abstract:** In the course of 248-nm laser flash photolysis, solutions of 9-phenylxanthen-9-ol (**1**) undergo homolytic and heterolytic photodehydroxylation, the relative efficiency of which depends strongly on the solvent nature. Polar/hydroxylic solvents, particularly aqueous mixtures, cause copious formation of 9-phenylxanthenium cation (**2**), the ground- and excited-state properties of which are conveniently studied by single- and double-laser flash photolysis. In 1:1 $H_2O$/MeCN, the quantum yield of carbenium ion generation is 0.4 ± 0.1; only 1% of photoheterolysis occurs through an adiabatic route. Surprisingly, in polar but nonhydroxylic solvents (e.g., acetonitrile and 1,2-dichloroethane) also, the cation is photogenerated in small but sufficient yields to allow time-resolved spectroscopic detection and study in these relatively neutral and inert media. In relatively nonpolar solvents, e.g., *n*-heptane and benzene, the photolysis of **1** is dominated by homolytic cleavage to 9-phenylxanthenyl radical (**3**). The short-lived triplets of **1** ($\tau_T \leq 0.3$ μs) are also observed in nonaqueous solvents ($\phi_T = 0.05$ in acetonitrile). In comparison to the weak, fast-decaying, doublet–doublet fluorescence of **3** ($\lambda_{max}^F = 590$ nm, $\tau_F \leq 5$ ns), the singlet–singlet fluorescence from **2** is intense and long-lived ($\lambda_{max}^F = 550$ nm, $\tau_F = 25$ ns in acetonitrile in the absence of nucleophilic quenchers) and is almost nonquenchable by oxygen ($k_q \leq 5 \times 10^8$ $M^{-1}$ $s^{-1}$). The electrophilicity of the lowest excited singlet state of **2**, measured in terms of rate constants ($k_q$) of bimolecular quenching by anions and lone-pair containing molecules, is considerably more pronounced than that of the ground state (that is, $k_q$'s are higher for the excited state by several orders of magnitude).

The cleavage of a carbon–heteroatom σ-bond as a result of the photoexcitation of a proximal π-system is of interest from several perspectives: First, the study of this photolytic event gives insight into the spatial factors that affect energy migration in the photoexcited state leading to chemical transformations. Second, the charge polarization in the excited-state potential surface, as controlled by intramolecular and environmental factors, manifests itself into heterolytic or homolytic bond cleavage, leading to ions or radicals.[3,4] The relative yields of the ionic and radical type

(1) The work described herein was supported by the Office of Basic Energy Sciences, Department of Energy. This is Document No. NDRL-3178 from the Notre Dame Radiation Laboratory.

(2) (a) Undergraduate research student (fall, 1987) from the University of Waterloo, Canada. (b) Present address: 347 PL, Phillips Research Center, Bartlesville, OK 74004.

(3) (a) Zimmerman, H. E.; Sandel, V. R. *J. Am. Chem. Soc.* **1963**, *85*, 915-922. (b) Zimmerman, H. E.; Somasekhara, S. *J. Am. Chem. Soc.* **1963**, *85*, 922-927.

(4) Turro, N. J.; Wan, P. *J. Photochem.* **1985**, *28*, 93-102.

0002-7863/89/1511-8858$01.50/0 